MEASUREMENT PROCEDURE OF RING MOTION WITH THE USE OF HIGH-SPEED CAMERA DURING ELECTROMAGNETIC EXPANSION

Jacek Janiszewski

Military University of Technology, Faculty of Mechatronics and Aviation, Kaliskiego 2, 00-908 Warsaw, Poland
(✉ jacek.janiszewski@wat.edu.pl, +48 22 683 7345)

Abstract

An optical measurement method of radial displacement of a ring sample during its expansion with velocity of the order 172 m/s and estimation technique of plastic flow stress of a ring material on basis of the obtained experimental data are presented in the work. To measure the ring motion during the expansion process, the Phantom v12 digital high-speed camera was applied, whereas the specialized TEMA Automotive software was used to analyze the obtained movies. Application of the above-mentioned tools and the developed measuring procedure of the ring motion recording allowed to obtain reliable experimental data and calculation results of plastic flow stress of a copper ring with satisfactory accuracy.

Keywords: high-speed camera, electromagnetic expanding ring test, high-strain-rate deformation.

1. Introduction

Various experimental techniques have been developed to study materials (also including nanomaterials [1]) at high-strain-rate loading conditions. The split Hopkinson pressure bar method is the most common [2-3], however, this technique has some limitations, so many other experimental methods were used to examine the dynamic behaviour of materials. These methods may include, among others, the impact Taylor test [4], a plate-on-plate impact test [5] and an expanding ring test [6]. All these experimental techniques require application of an advanced measuring system being able to measure some quantities during the deformation process, which occurs for a very short time. The most distinct examples of such a highly-advanced measurement system is the Velocity Interferometer System for Any Reflector (VISAR) [7], which is often used in a plate-on-plate impact experiment to record the velocity profile of a free surface [8]. During this experiment, the free surface of a shock loaded plate moves with a velocity of the order of hundreds of metres per second and the whole phenomenon occurs only for a period of a few microseconds [9].

In the study of dynamic behavior of materials in expanding ring loading conditions, the VISAR system has been also applied to measure the velocity history of ring expansion. This measuring system is very appropriate for this purpose, however, it creates technical and methodological difficulties and, in addition, it is very expensive. Therefore, only a few laboratories are capable of performing this test. For this reason, the alternative measuring systems for recording the ring motion have been searched. Recently, Zhang and Ravi-Chandar used an innovative high-speed camera system to obtain high-spatial resolution images showing ring deformation and the fragmentation process [9]. Through perfect quality images, they were able not only to determine the velocity expansion profile, but they could also observe multiple necks nucleate along the circumference of the ring and a propagation shock wave generated by an electric arc. Besides the above mentioned unique camera system,

different digital high-speed cameras are also available on the market. The present-day digital optical recording systems are able to observe the history of ultra-fast events with a time resolution at least of 1 μs. However, these cameras have limitations, which are the result of a low optical resolution for high frame rates or a small amount of frames. For example, the Vision Research Phantom v711 high-speed camera guarantees a maximum frame rate of 1,400,000 frames-per-second (fps), while at a reduced optical resolution to 128 x 8 pixels [10].On the other hand, the DRS Imacon 200 ultra-high-speed digital camera takes pictures with a high resolution of 1280 x 1024 pixels and with a frame rate of 200 million fps, but the maximum number of frames is only up to 16 [11].

Despite the above-mentioned limitations of modern digital high-speed camera systems in the present work, there was an attempt made to use the Phantom v12 high-speed camera for recording the ring motion history. The satisfactory accuracy of the ring position during expansion was obtained with the use of a special measuring procedure, which was developed and adapted to conditions of an electromagnetic expanding ring test.

The paper is organized as follows: Section 2 is devoted to the description of materials study methodology with the use of an electromagnetic expanding ring test and the laboratory apparatus developed at the Military University of Technology. The recording method of ring expansion using the Phantom v12 high-speed camera and the analysis of the obtained experimental data performed with the use of the Tema Motion 2D software are described in Section 3. The calculation results of plastic flow stress for ring material and discussion on the influence of ring width changes during expansion on the calculated flow stress data are also presented in Section 3.

2. Expanding ring technique

2.1. Essence of expanding ring test

The expanding ring test is based on recording of the motion of the thin-walled ring made from the tested material, which was launched due to detonation of an explosive charge or electromagnetic impulse loading. After an acceleration stage, the ring rapidly becomes a free-flying body and decelerates due to its own internal circumferential stresses (Fig. 1).
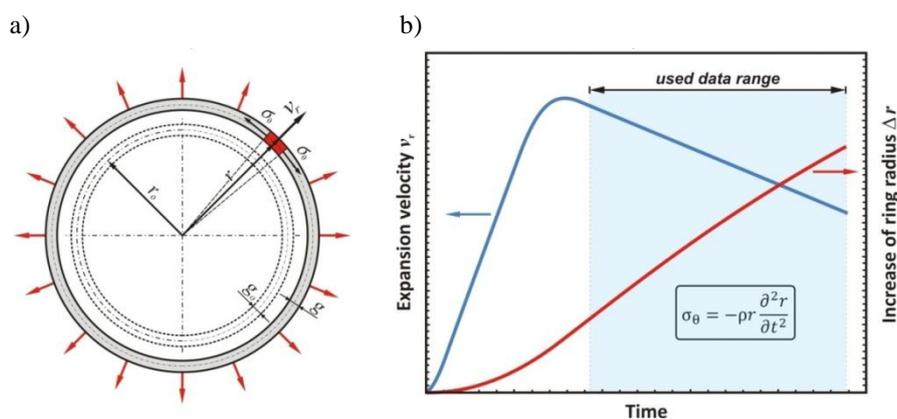

Fig. 1. Schematic illustration of ring expansion (a) and curves of radial displacement and velocity expansion (b), where g_o and g denote the initial and current width of the ring, respectively.

By measuring the radius r or expansion velocity v_r of the ring specimen during the inertial stage of expansion, the circumferential stress σ_θ, true strain ε_θ and strain rate $\dot{\varepsilon}_\theta$ for the ring material can be determined at the imposed strain rate using the following relationships:

$$\sigma_\theta = -\rho r \frac{\partial^2 r}{\partial t^2}, \tag{1}$$

$$\varepsilon_\theta = \int_{r_o}^{r} \frac{dr}{r} = \ln\frac{r}{r_o}, \tag{2}$$

$$\dot{\varepsilon}_\theta = \frac{v_r}{r}. \tag{3}$$

where: ρ – density of a sample material cylinder, r_o and r – initial and current radius of a ring specimen, v_r – current expansion velocity, respectively.

2.2. Laboratory apparatus for electromagnetic ring expansion

The idea of electromagnetic metal ring expansion was taken from an original design proposed by Niordson [12]. In accordance with it, a ring specimen made of the tested material is placed concentrically over a mandrel containing a wire coil (Fig. 2). At the beginning, a capacitor bank is charged to a high voltage *V* and next rapidly discharged through the wire solenoid and a magnetic field is produced around the coil. Simultaneously, this magnetic field induces an oppositely directed current in the metal ring specimen, which generates a magnetic field as well. As a result of interaction between the magnetic fields originated by the coil and ring currents, uniform radial body forces are created. These forces, applied for a very short time, accelerate the ring specimen to high velocity and next they vanish when the solenoid current drops to a low value. Since that time the ring continues the expansion only by its inertia. If the inertia forces are large enough, the ring can fracture into several small fragments.
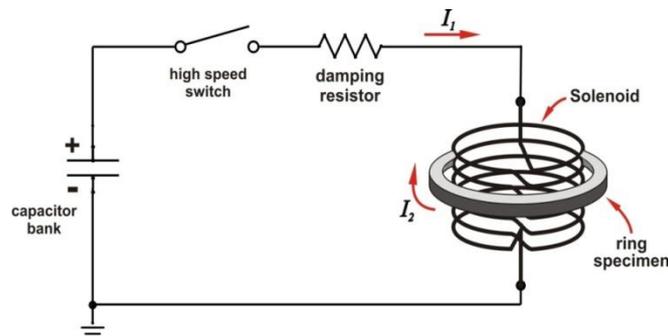

Fig. 2. Schematic diagram of the arrangement for electromagnetic ring expansion.

The arrangement for electromagnetic ring expansion applied in the present work is based on the construction proposed in Gourdin's works [13-14]. A view of the device for electromagnetic launch of the ring specimen is shown in Fig. 3, and its extended description is presented in [15].

Principally, this apparatus consists of three main components; *a pulse power system* containing a 240 µF capacitor bank and two impulse thyristors, *a loading assembly*, and *a charging system*. A solenoid with a ring sample is inserted into the loading assembly. It consists of two transparent plates with cavities, which support the solenoid with the copper ring and a wax gel ring at the outside of the cavity. The wax gel ring plays the role of a capture medium for fragments generated during fracture of the ring sample.

The solenoid and ring samples were developed to be close to dimensions used by Grady and Benson [16] and Gourdin *et. al* [13]. The solenoid consists of 6 turns of 1.3-mm copper wire wound without pitch (except for a narrow transition strip) on a polycarbonate mandrel fitted to the dimension of the ring specimen. The cross-sectional area of the ring was equal to 1 mm x 1 mm, whereas the mean ring diameter was 32 mm. The ring samples were machined

from a cold-rolled Cu-ETP copper bar with a 40-mm diameter. Particular attention was paid to ensuring a sufficiently high dimensional accuracy and surface quality of the ring samples. The rings used in the present work were manufactured with a dimensional tolerance of ±0.01 mm, whereas the ring surface roughness defined here by parameter Ra was not higher than 1.2 µm.
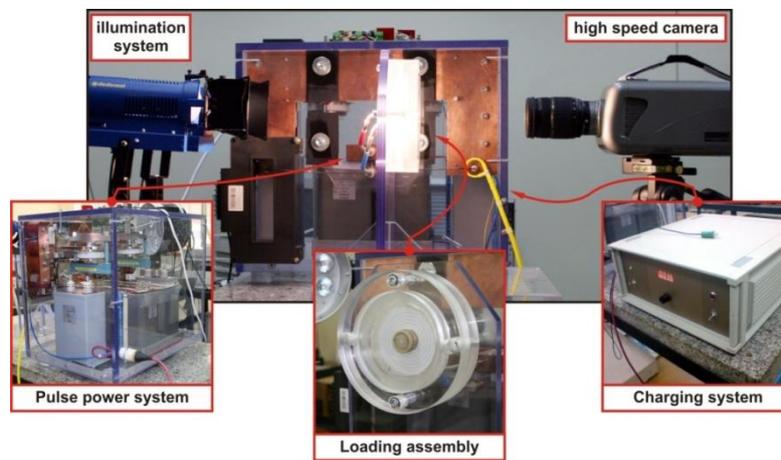

Fig. 3. View of the arrangement for electromagnetic ring expansion.

3. Recording procedure of ring expansion

The construction of the loading assembly was adjusted to optical records of the ring motion. Therefore, the front plate was transparent whereas the rear plate was also transparent but with a matt surface. Displacement of the ring during the expansion process was recorded with the Phantom v12 high-speed camera (Fig. 3), which guarantees achieving images with a frame rate of 1,000,000 fps, however, with a low optical resolution (128 x 8 pixels).

In order to obtain good-quality images and to ensure a satisfactory measuring accuracy of the ring displacement with the use of the available equipment, first of all, a shadow method of optical observation was applied. This method consists in recording of a ring shadow on a highlighted background, which is illuminated by a Dedocool lighting system [17] (Fig. 3) allowing concentration of an intense amount of light over a small area. For example, the selected images of the ring during its radial expansion were collected in Fig. 4. In the central part of the image in Fig. 4, the coil and the ring are visible; they were initially at the periphery of the solenoid in the symmetry plane between the third and the fourth coil turn. Upon discharge of a current pulse through the coil, the ring expands radially, and next it fractures into several fragments. It should be noted here that the white stains in the images 120 µs and 180 µs originate from electric arcs emerging at fracture points as a result of high current circulation of in the ring during its fragmentation process.
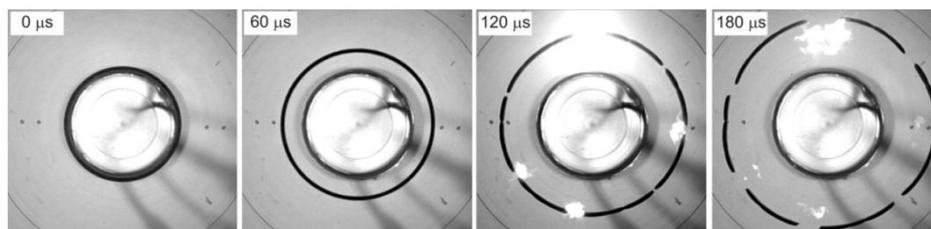

Fig. 4. The sequence of images showing the ring expansion process.

www.czasopisma.pan.pl   PAN   www.journals.pan.pl
POLSKA AKADEMIA NAUK

Metrol. Meas. Syst., Vol. XIX (2012), No. 4, pp. 797-804.

The images presented in Fig. 4 are not sufficient enough, however, to obtain complete information on the ring motion during expansion. For this recording configuration, the optical resolution was 256 x 256 pixels and images were taken with a frame rate of 66,037 fps, what means that images were recorded in the period of 15.14 μs. Thus, all the ring expansion process, which lasted about 60 μs, was represented only by four images, what is not enough to determine the curves describing changes of the ring radius or ring velocity during expansion. Therefore, the observation field of a high-speed camera was limited to a small area in which only a moving ring segment and two scaled points were visible (Fig. 5a). The optical resolution of the observation field was 256 x 32 pixels, and the images were recorded with a time interval of 2.38 μs (frame rate – 421,052 fps). In this case, the ring expansion was recorded in about 25 images. It is a sufficient number of images to assess the ring expansion motion, but the optical resolution is too low to guarantee appropriate measuring accuracy. Therefore, the Tema Automotive software [18] was used which allowed the achievement of a high enough measuring accuracy (uncertainty of ±0.01 mm for the results presented here) and obtainment of reliable data on the ring expansion history (Fig. 5b).
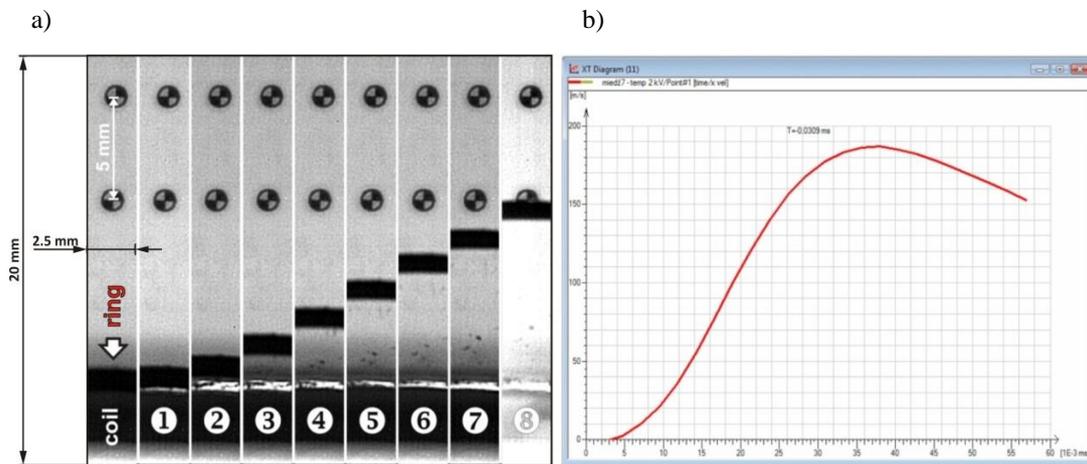

Fig. 5. The sequence of images showing the observation area with the moving ring segment (a) and the example of screen shot of the expansion velocity curve calculated from images with the use of TEMA Automotive software (b).

It should be noted here that most of investigators have determined the function $r(t)$ or $v_r(t)$ based on observation of a point which is situated on the external surface of the ring specimen. In the case of the VISAR measuring system, it is the only way to measure the ring expansion. However, the motion of the external ring surface is not only the result of changes of the mean ring radius, but also the result of changes of its width g. This fact is usually ignored, because changes of ring width g during the ring expansion process are relatively small in comparison to the changes of the ring radius, and therefore it is believed to have a slight influence on the final results of plastic flow stress calculation for the ring material. In the present work, it was decided to find the real influence of changes of the ring width on the value of plastic flow stress of the ring material.

In order to solve the above problem, some useful features of the Tema Automotive software were applied, namely, the capability of tracking of any points through the image sequence with subpixel accuracy. In Fig. 6, screenshots are presented showing the position of the tracking points in relation to the ring sample surfaces. The first point is situated on the external ring surface, the second one in the mean ring radius, whereas the third one is joined with the internal ring surface. The curves of position changes of these points during ring expansion were also included in Fig. 6. These curves are representative data for three experiments which were performed for a copper ring with a discharge energy of 0.48 kJ. The

obtained averaged maximum ring expansion velocity was 172 m/s, which corresponds to a strain rate level of 8×10^3 s^{-1}.

For the received experimental curves, the corresponding functions $r(t)$ were determined, however, a parabolic approximation was applied in accordance of the suggestion proposed by Hoggatt and Recht [19]. The forms of the determined functions $r(t)$ and the results of flow stress calculation (1) for a strain of 0.25 were collected in Fig. 6 as well. It should be emphasized here that for the experimental curves of position changes of the observation points, excellent data fitting was received with a coefficient of determination of R^2 equal to 0.9999 (values of R^2 were calculated with the use of a standard procedure offered by Mathcad software).

The results presented in Fig. 6 allow to claim that the history of the ring radius during expansion is slightly different depending on the position of the tracking point. It is demonstrated by a little difference between coefficient values of approximation equations determined for the given tracking point. For tracking point (1), function $r(t)$ takes form as follows: $r(t)_1 = -1018012.5\, t^2 + 237.0\, t - 2.9$, whereas for tracking points (2) and (3) formulas of function $r(t)$ are given by: $r(t)_2 = -1077408.1\, t^2 + 242.2\, t - 3.5$ $r(t)_3 = -1091209.4\, t^2 + 245.0\, t - 4.1$, respectively. As a consequence, the values of plastic flow stress, being a result of double differentiation of the approximation equations, also varied. For the tracking point situated on the internal surface (3), calculated plastic flow stress was the highest ($\sigma_\theta = 403.7$ MPa), for the external tracking point (1) – the lowest (($\sigma_\theta = 376.6$ MPa), whereas for the mean tracking point (2),which is not affected by the changes of the ring width during expansion, the stress of σ_θ achieved the value of 398.6 MPa. Similar relations were obtained for the other experiments (Table 1).

Thus, the position of the tracking point has a slight influence on the accuracy of experimental data describing the history of the ring expansion. It is also proved by low values of the relative error, which was calculated for a real value represented by the average taken from values of flow stresses determined for tracking point (2). Hence, a relative error for plastic flow stress calculated on the basis of the $r(t)$ curve for tracking point (3) (external surface) was, on the average 1.85%, while for the tracking point situated on the internal surface (1) it was slightly higher and equal to 4.7%. This higher error for tracking point (1) seems to be, probably, the result of a streak effect, which is usually observed when recording a fast-moving object.
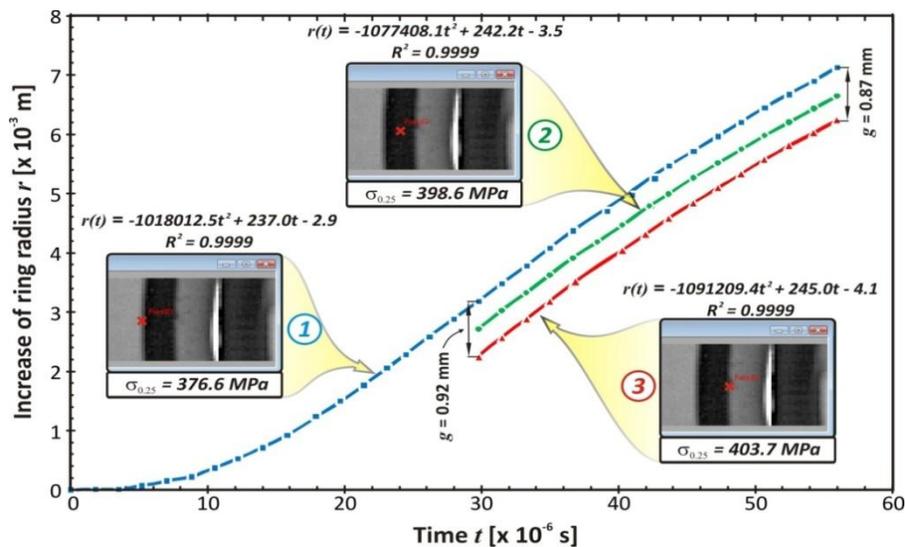

Fig. 6. The influence of position of the tracking point on the calculation of plastic flow stress of the ring material.

Table 1. Calculation results for electromagnetic expansion experiments.

Test number	Tracking point	Deceleration $\frac{\partial^2 r}{\partial t^2}$ [m/s^2]	Flow stressσ_θ for $\varepsilon_\theta = 0,25$ [MPa]	Maximum expansion velocity [m/s]	Strain rate for $\varepsilon_\theta = 0.25$ [s^{-1}]
No. 01	1	2032122	**376**		
	2	2119788	**392**	173,1	7,66 x 10^3
	3	2169746	**401**		
No. 02	1	2036025	**377**		
	2	2154816	**399**	171,7	7,61 x 10^3
	3	2182419	**404**		
No. 03	1	2050765	**379**		
	2	2144279	**397**	172,2	7,63 x 10^3
	3	2187894	**405**		

4. Conclusions

The optical measurement method of radial displacement of a ring sample during electromagnetic expansion with the use of a digital high speed camera system was described. Due to the developed procedure of ring observation and application of the Tema Automotive software, a relatively high accuracy of ring position measurement was achieved during expansion with the radial velocity of the order of 170 m/s. Moreover, it was found that the small influence of the ring width changes during its plastic deformation on the function form of $r(t)$. Thus, determination of curve $r(t)$ based only on the observation of motion of the tracking point situated on the external ring surface contributes a small error (relative error $< 2\%$) to the value of plastic flow stress.

Acknowledgements

References

[1]   Kurzydlowski, K.J. (2010). Modelling of the microstructure and properties in the length scales varying from nano- to macroscopic. *Bull. Pol. Acad. Sci.-Tech. Sci*, 58(2), 217-226.

[2]   Klepaczko J. (2007). *Introduction to experimental techniques for materials testing at high strain* rates. Institute of Aviation Scientific Publications Group, Warsaw.

[3]   Weinong W. Chen, Bo Song. (2010). Split Hopkinson (Kolsky) Bar: *Design*, *Testing* and *Applications*. Springer New York-Dordrecht-*Heidelberg-London.*

[4]   Taylor G. (1948). The use of flat-ended projectiles for determining dynamic yield stress I. Theoretical considerations. *Proc. Roy. Soc. London Series A*, 194, 289.

[5]   Asay J.R. (1997). The use of shock-structure methods for evaluating high-pressure material properties. *International Journal of Impact Engineering*, 20, 27-61.

[6]   Johson P.C., Stein B.A., Davis R.S. (1963). Measurement of Dynamic Plastic Flow Properties Under Uniform Stress. *Symposium on the Dynamic Behavior of Materials*, *ASTM Special Publication*, 336.

[7]   Asay J.R., Barker L.M. (1974). Interferometric measurement of shock-induced internal particle velocity and spatial variations of particle velocity. *Journal of Applied Physics*, 45(6).

[8]   Field J.E., Pround W.G., Walley S.M., Goldrein H.T., Siviour C.R. (2004). Review of experimental techniques for high rate deformation and shock studies. *International Journal of Impact Engineering*, 30, 725-775.

[9]   Zhang H., Ravi-Chandar K. (2006). On the dynamics of necking and fragmentation – I. Real-time and post-mortem observations in Al 6061-O. *Int. J. Fract.*, 142, 183-217.

[10]   *http://www.visionresearch.com/Products/High-Speed-Cameras/v121/* (Jan. 2012).

[11]   *http://www.itronx.com/pdf/DRS_Imacon_200.pdf* (Jan. 2012).

[12]   Niordson F.I. (1965). A unit for testing Materials at High Strain Rates. *Experimental Mechanics*.

[13]   Gourdin W.H., Weinland S.L., Boling R.M. (1989). Development of the electrometrically launched expanding ring as a high-strain-rate test technique. *Rev. Sci. Instrum*., 60(3), 427-432.

[14]   Gourdin W.H. (1989). Analysis and assessment of electromagnetic ring expansion as a high-strain-rate test. *J. Appl. Phys.*, 65(2), 411-422.

[15]   Janiszewski J., Pichola W. (2009). Development of Electromagnetic Ring Expansion Apparatus for High-Strain-Rate Test, *Solid State Phenomena*, 147-149, 645-650.

[16]   Grady D.E., Benson D.A. (1983). Fragmentation of metal Rings by Electromagnetic Loading, *Experimental Mechanics*, 23.

[17]   *http://www.dedolight.com* (January 2012).

[18]   *http://www.imagesystems.tv/motion-bu/products/tema-automotive.aspx* (Jan. 2012).

[19]   Hoggatt C.R., Recht R.F., (1969). Stress-strain data obtained at high rates using an expanding ring, *Experimental Mechanics*, 9, 441-448.